Supplementary Information (SI) for Nanoscale.
This journal is © The Royal Society of Chemistry 2024

Supplementary Information for

The dual-functional role of carboxylate in a nickel-iron catalyst towards efficient oxygen evolution

Dan Wu, Yuanhua Sun, Xue Zhang, Xiaokang Liu, Linlin Cao* and Tao Yao

National Synchrotron Radiation Laboratory, School of Nuclear Science and Technology, University of Science and Technology of China, Hefei 230029, P.R. China.

E-mail: caolin@ustc.edu.cn

Supplementary Figures

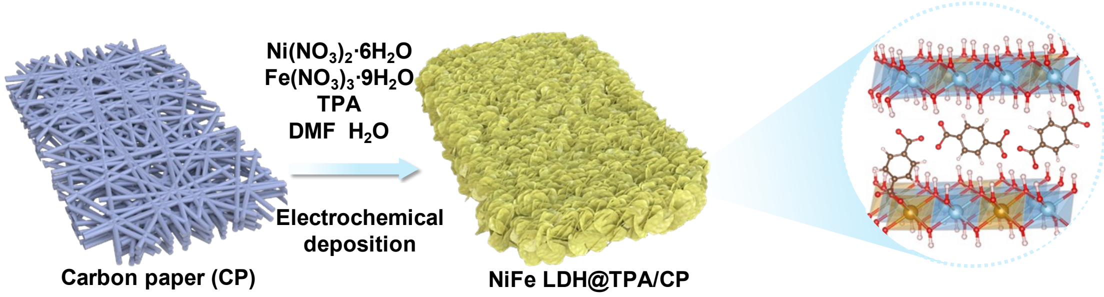

Fig. S1 The schematic diagram of the synthesis process for NiFe LDH@TPA electrode.

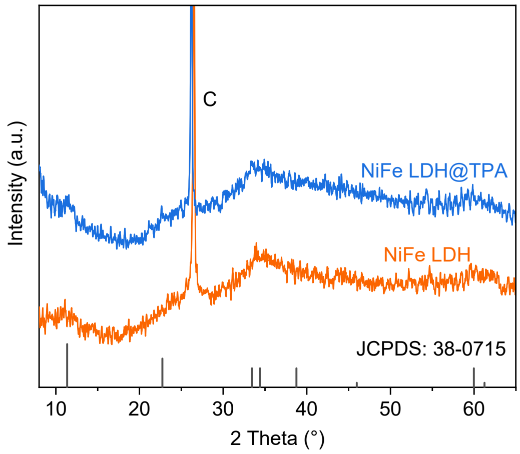

Fig. S2 XRD patterns of NiFe LDH and NiFe LDH@TPA. The sharp diffraction peak at about 26° is originated from the carbon in the carbon paper.

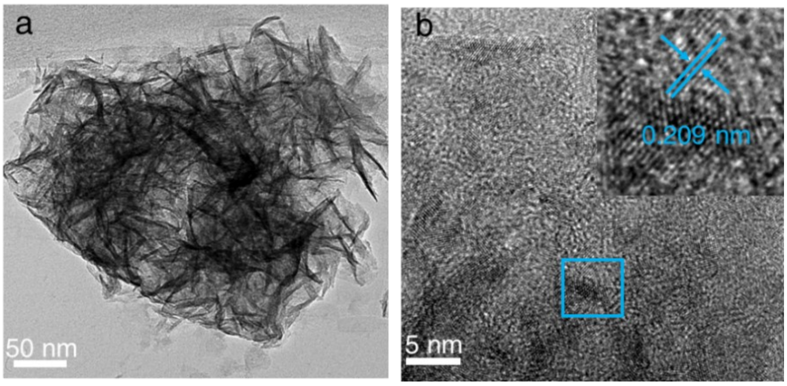

Fig. S3 (a) TEM and (b) HRTEM images of NiFe LDH.

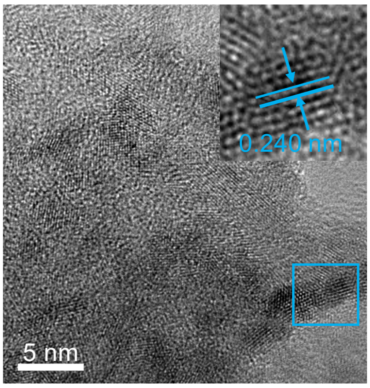

Fig. S4 HRTEM images of NiFe LDH@TPA.

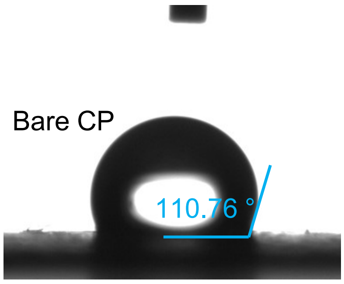

Fig. S5 The contact angles of bare CP.

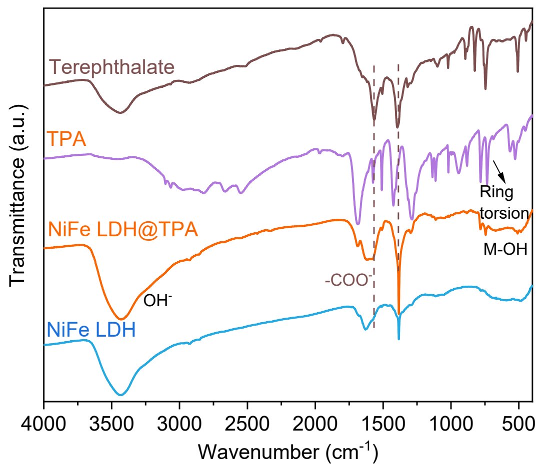

Fig. S6 FTIR spectra of NiFe LDH, NiFe LDH@TPA, and reference samples in the range of 400-4000 cm^{-1}.

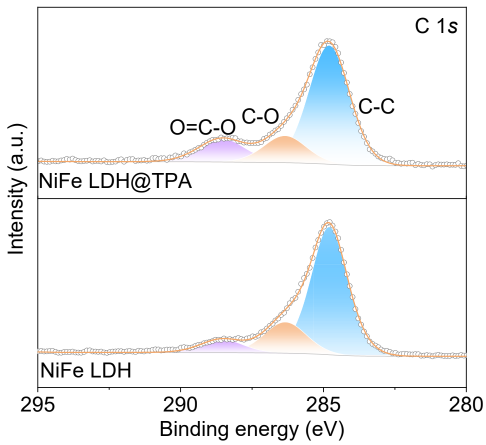

Fig. S7 C 1*s* high-resolution XPS spectra of NiFe LDH@TPA and NiFe LDH.

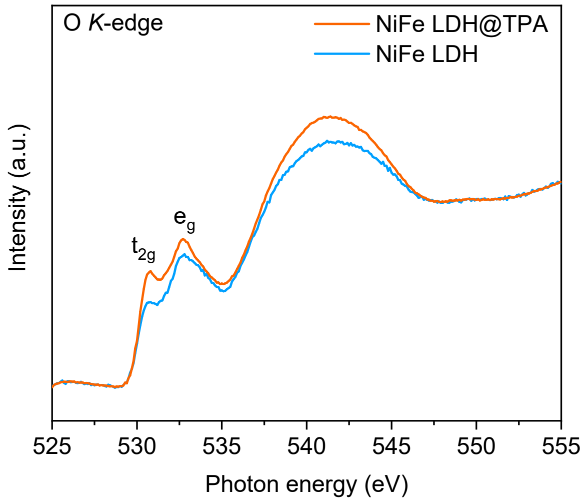

Fig. S8 O *K*-edge sXAS spectra of NiFe LDH@TPA and NiFe LDH.

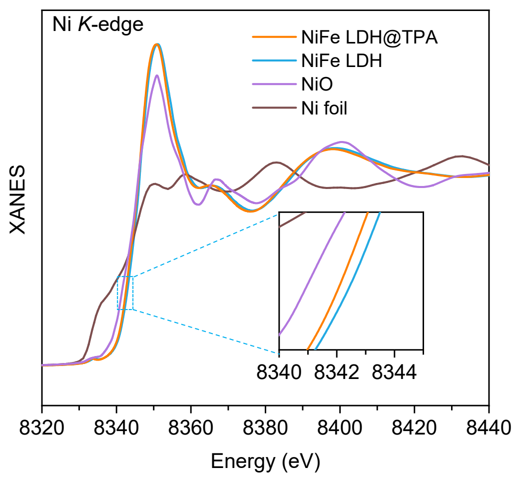

Fig. S9 Ni *K*-edge XANES spectra of NiFe LDH@TPA, NiFe LDH, and referenced samples.

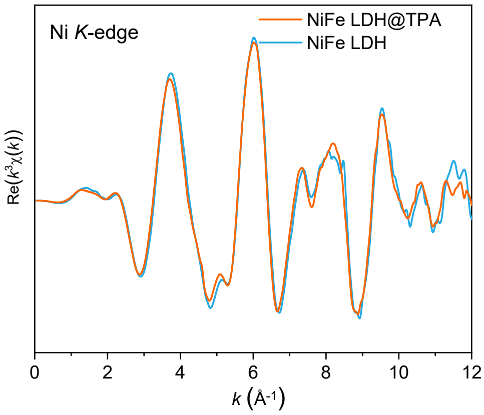

Fig. S10 $k^3\chi(k)$ oscillations spectra of Ni *K*-edge of NiFe LDH@TPA, NiFe LDH.

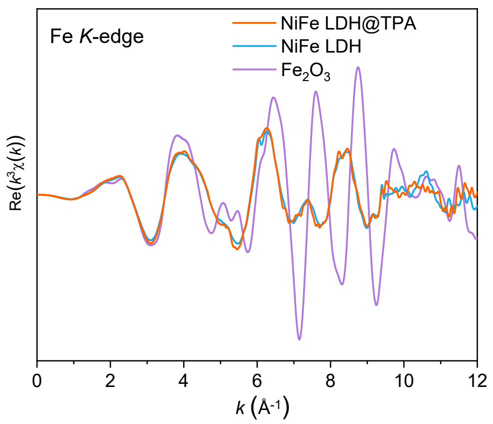

Fig. S11 $k^3\chi(k)$ oscillations spectra of Fe K-edge of NiFe LDH@TPA, NiFe LDH and referenced sample.

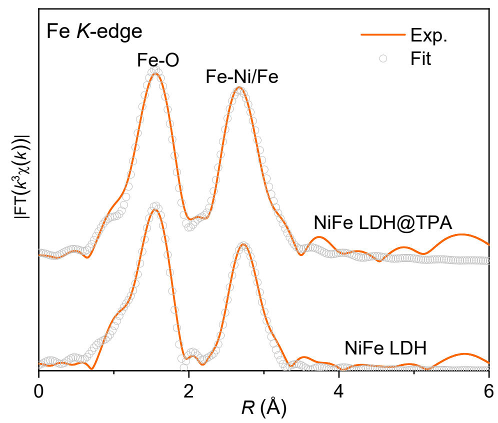

Fig. S12 Fe *K*-edge FT-EXAFS curves and corresponding fitting of NiFe LDH@TPA and NiFe LDH.

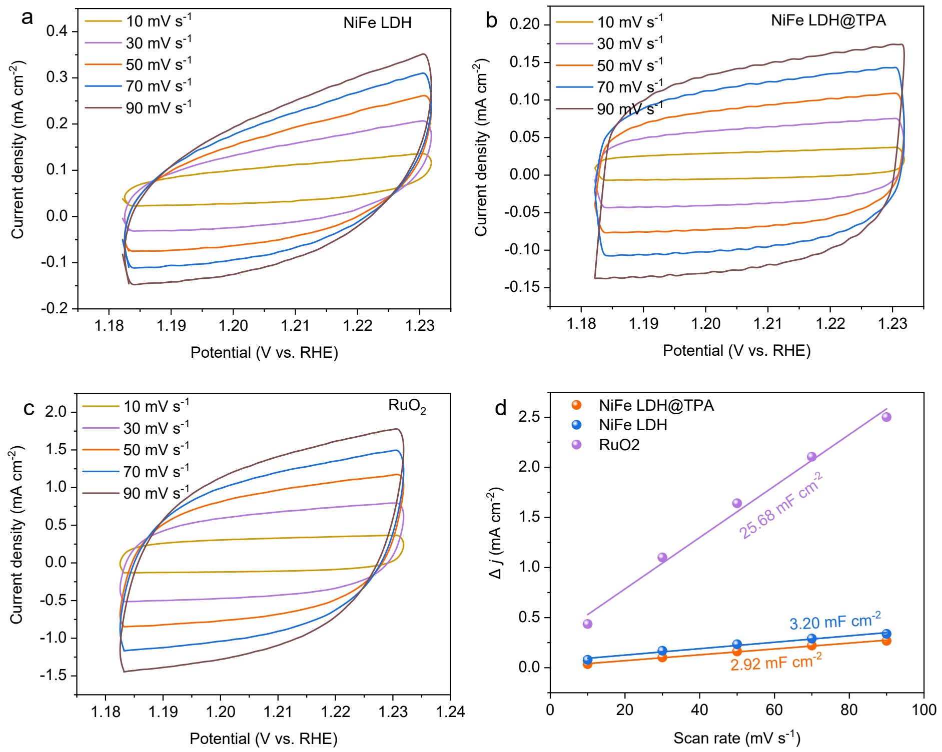

Fig. S13 Cyclic voltammograms (CVs) recorded within a non-faradaic region at different scan rates for (a). NiFe LDH, (b) NiFe LDH@TPA, and (b) RuO_2. (d) Double-layer capacitances (C_{dl}).

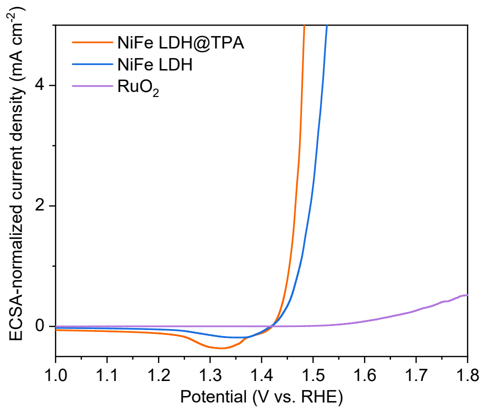

Fig. S14 The ECSA-normalized LSVs of the electrocatalysts.

The ECSA of electrocatalyst was estimated from the obtained double-layer capacitances (C_{dl}) according to the formula:

$$ECSA = C_{dl}/C_s \qquad \text{(Eq. S1)}$$

The C_{dl} value was calculated from related cyclic voltammograms (CVs), which were recorded within a non-faradaic region at different scan rates. The term C_s stands for the specific capacitance of a smooth surface per unit area under certain circumstances. In this work, a C_s value of 0.04 mF cm^{-2} was used.

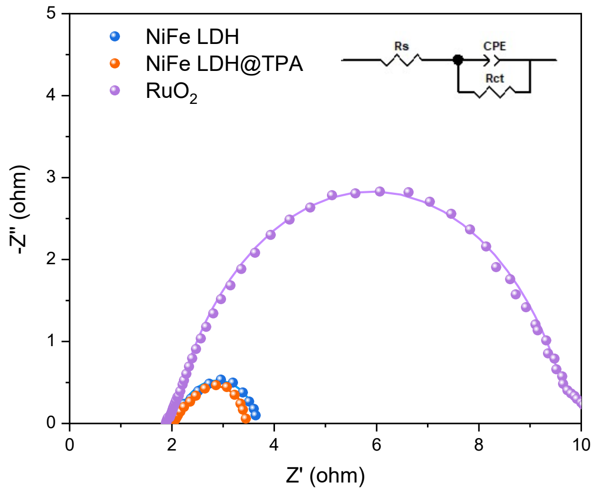

Fig. S15 Nyquist plots for the prepared catalysts and the Equivalent circuit for the fitting of the EIS responses. The solid lines represent corresponding fitting curves. R_s, R_{ct}, and CPE represent the series resistance, charge-transfer resistance, and constant phase elements, respectively.

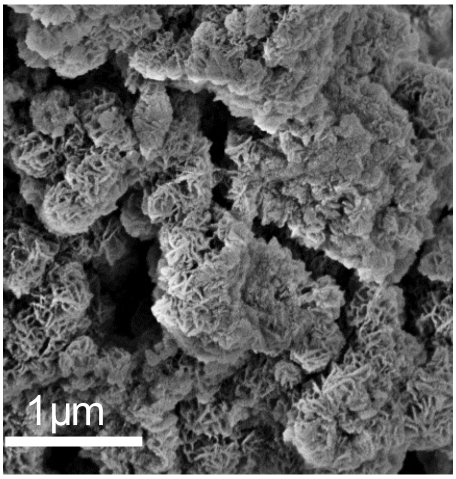

Fig. S16 SEM image of NiFe LDH@TPA after durability test.

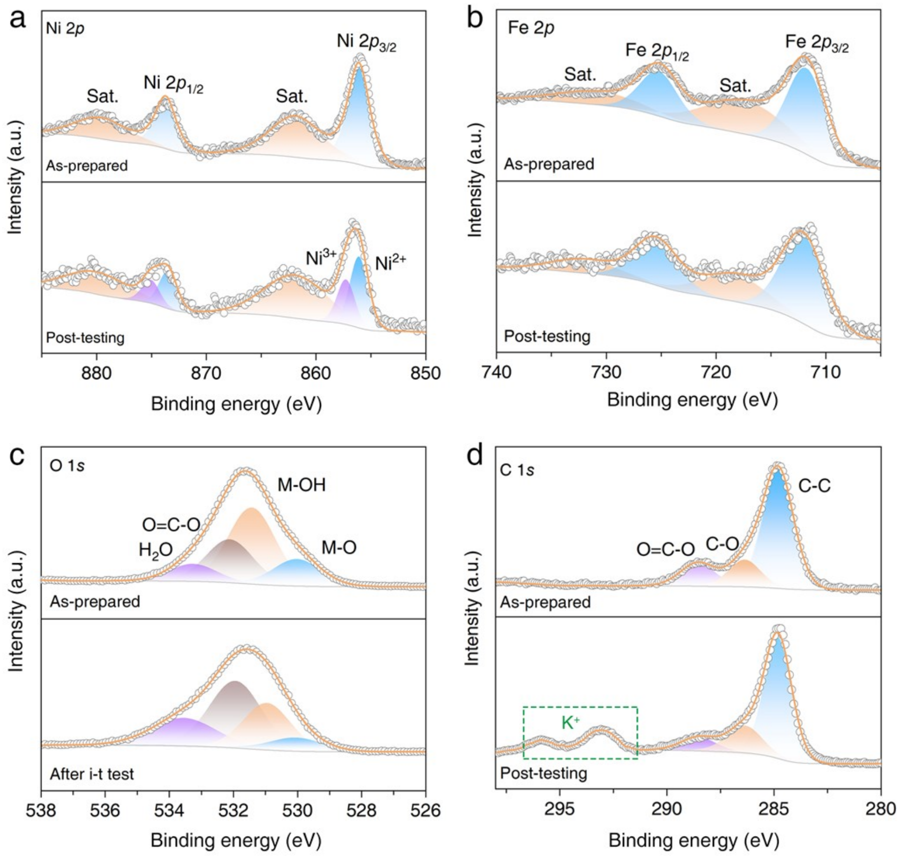

Fig. S17 (a) Ni 2*p*, (b) Fe 2*p*, (c) O 1*s*, and (d) C 1*s* XPS spectra of as-prepared and post-testing NiFe LDH@TPA. The XPS peaks located at around 293 and 296 eV are attributed to the K^+ from the electrolyte.

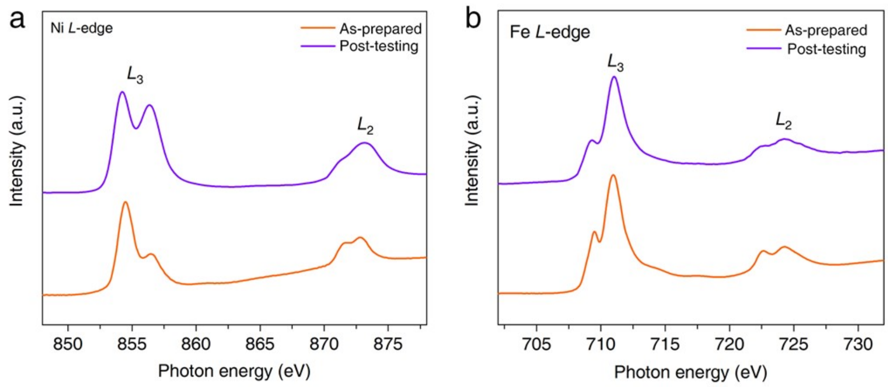

Fig. S18 sXAS spectra of as-prepared and post-testing NiFe LDH@TPA recorded at (a) Ni and (b) Fe *L*-edge.

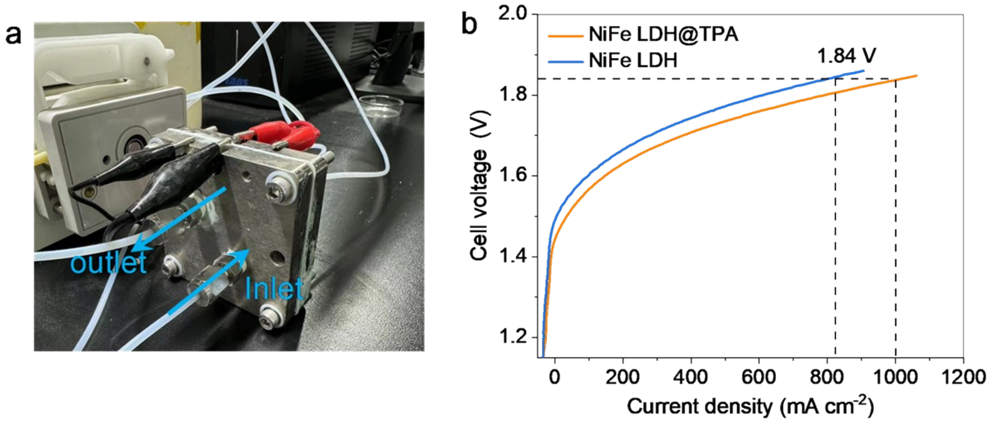

Fig. S19 (a) The photograph of AEMWE for the test. (b) Polarization curves in the AEMWE operated at 60 °C and 1 M KOH.

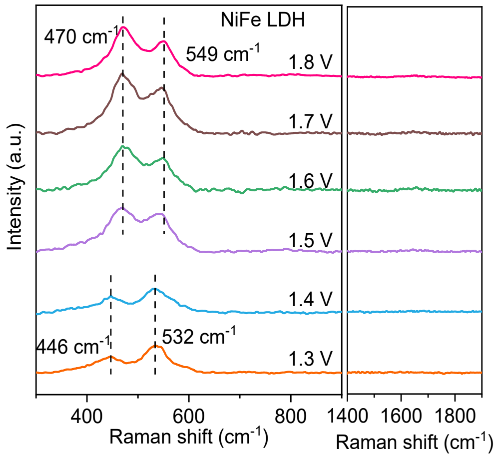

Fig. S20 *In situ* Raman spectra of NiFe LDH.

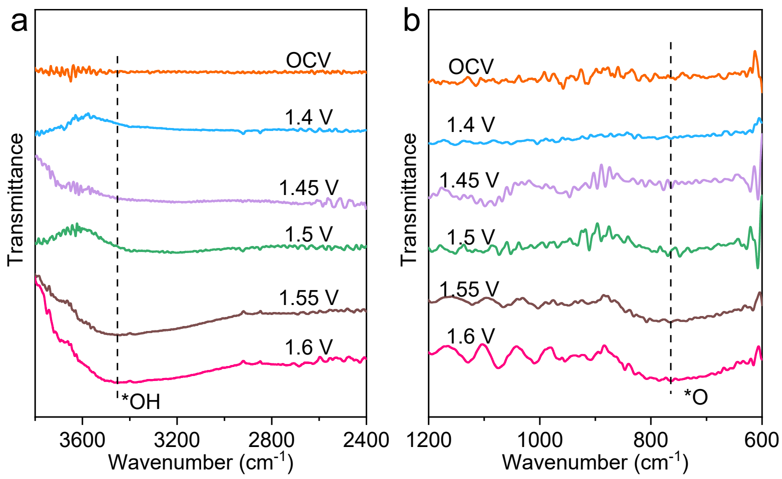

Fig. S21 *In situ* SRIR spectra of NiFe LDH.

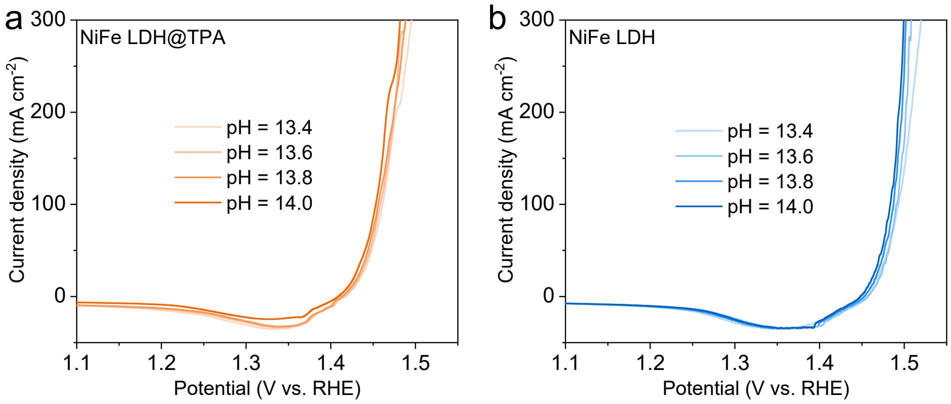

Fig. S22 pH-dependent LSV curves of (a) NiFe LDH@TPA and (b) NiFe LDH.

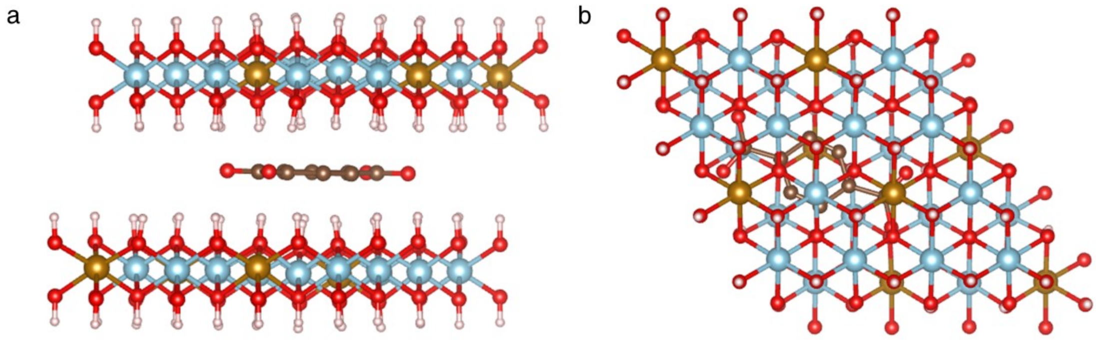

Fig. S23 The optimized configurations of NiFe LDH@TPA for DFT calculation.

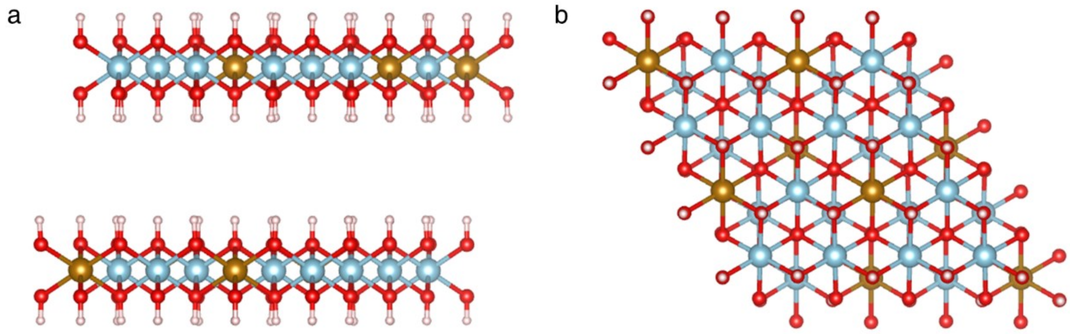

Fig. S24 The optimized configurations of NiFe LDH for DFT calculation.

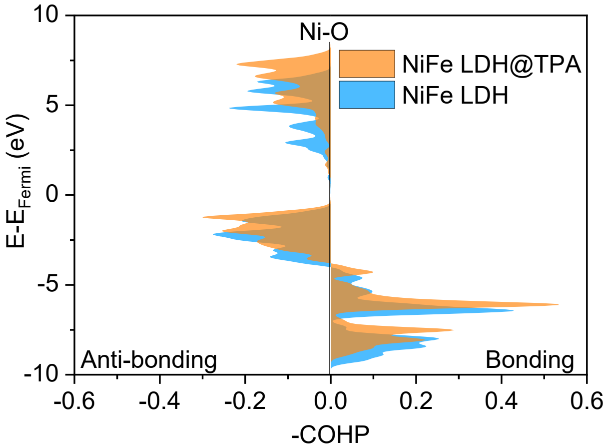

Fig. S25 -COHP of Ni-O bond in NiFe LDH@TPA and NiFe LDH. The –ICOHP values of Ni-O bond in NiFe LDH@TPA and NiFe LDH are 0.48 and 0.43, respectively.

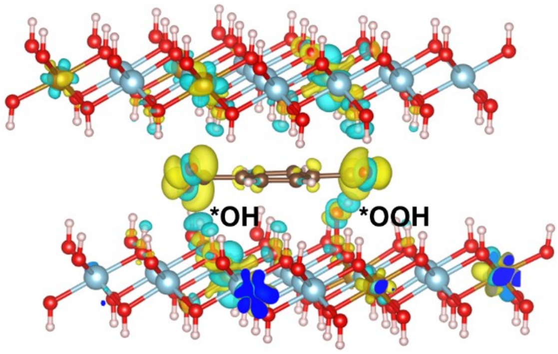

Fig. S26 Charge density difference analysis between *OH and *OOH intermediates and TPA in NiFe LDH@TPA.

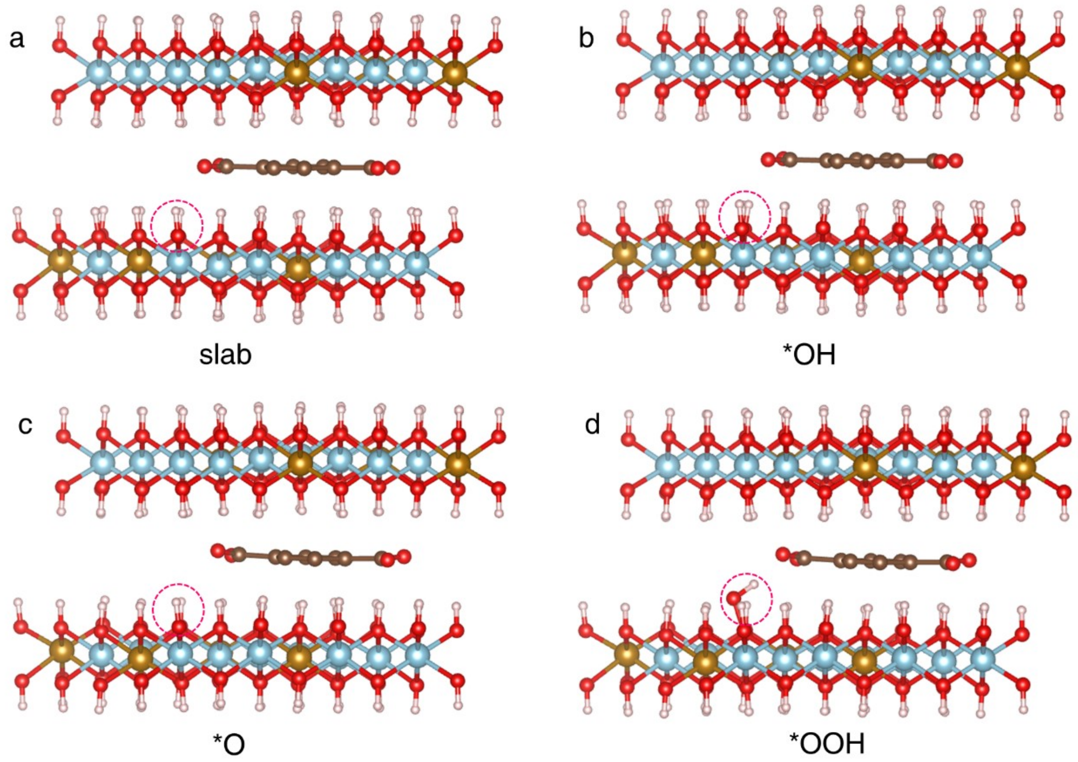

Fig. S27 The optimized configurations of *OH, *O, and *OOH adsorbed on NiFe LDH@TPA.

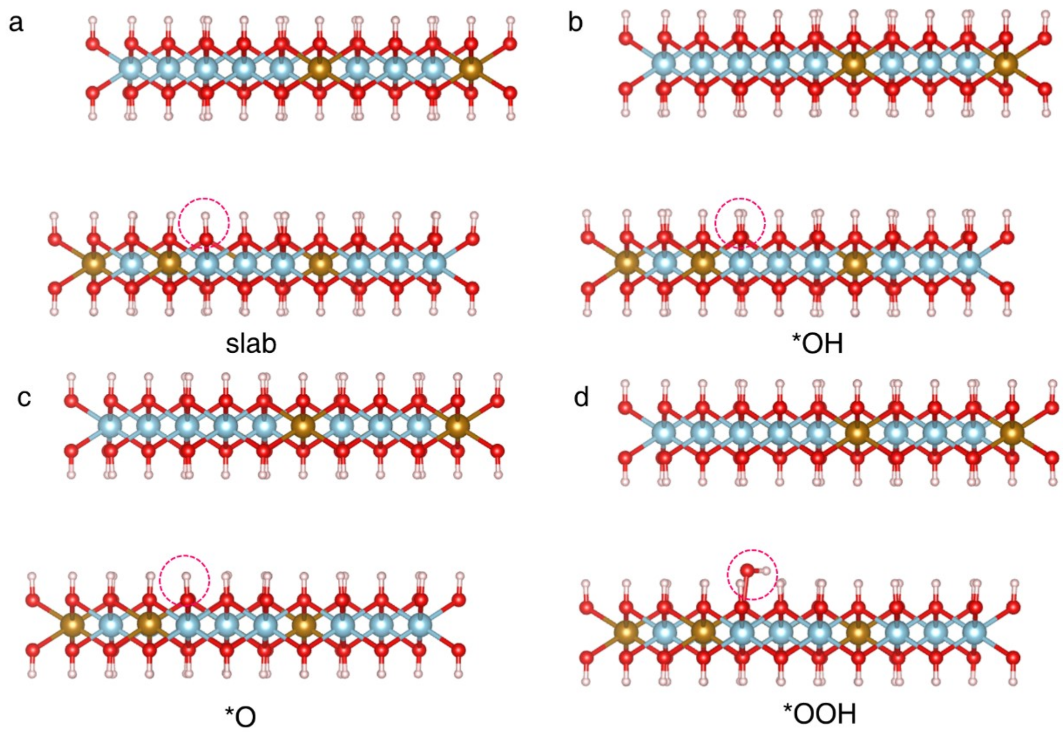

Fig. S28 The optimized configurations of *OH, *O, and *OOH adsorbed on NiFe LDH.

Table S1 Structural parameters extracted from the Ni and Fe *K*-edge EXAFS fitting.

			Ni *K*-edge			
Sample	**Path**	**CN**	**R(Å)**	**$\sigma^2(10^{-3}Å^2)$**	**ΔE_0 (eV)**	**R-factor**
NiFe LDH@TPA	Ni-O	6.02	2.048	6.55	-2.85	0.009
	Ni-Ni/Fe	5.50	3.098	10.57	1.56	
NiFe LDH	Ni-O	6.04	2.049	6.05	-1.50	0.007
	Ni-Ni/Fe	5.09	3.099	10.02	2.12	
			Fe *K*-edge			
Sample	**Path**	**CN**	**R(Å)**	**$\sigma^2(10^{-3}Å^2)$**	**ΔE_0 (eV)**	**R-factor**
NiFe LDH@TPA	Fe-O	5.41	1.998	6.30	-4.76	0.006
	Fe-Ni/Fe	5.31	3.110	8.58	-3.14	
NiFe LDH	Fe-O	5.32	2.001	5.76	-4.82	0.007
	Fe-Ni/Fe	5.38	3.111	9.43	-3.94	

S_0^2 is the amplitude reduction factor (0.78 for Ni; 0.85 for Fe); *CN* is the coordination number; *R* is interatomic distance (the bond length between central atoms and surrounding coordination atoms); σ^2 is Debye-Waller factor (a measure of thermal and static disorder in absorber-scatterer distances); ΔE_0 is edge-energy shift (the difference between the zero kinetic energy value of the sample and that of the theoretical model). *R* factor is used to value the goodness of the fitting.

Table S2 The parameters for the fitting of the EIS.

Catalysts	**$R_s(\Omega)$**	**$R_{ct}(\Omega)$**
NiFe LDH@TPA	1.973	1.697
NiFe LDH	1.997	1.849
RuO_2	1.95	7.904

Table S3 Comparison of the overpotentials at 10 mA cm^{-2} and Tafel slopes among different electrocatalysts under alkaline OER.

Catalysts	η@10 mA cm^{-2} (mV)	Tafel slope (mV dec^{-1})	Reference
NiFe LDH@TPA	200	29.2	This work
Au_{SA}-MnFeCoNiCu LDH	213	27.5	Ref [1]
Co-Fe catalyst	319	28.3	Ref [2]
γ-FeOOH/Ni-MOFNA	193	36	Ref [3]
NiFe-ANR	228	37	Ref [4]
Ir_1/V_{O}-CoOOH	200	32	Ref [5]
Fe-NiO/NiS_2	270	40	Ref [6]
MIL-53(Fe)-2OH	215	45.4	Ref [7]
Mo_1-$NiFeO_xH_y$	193	32.33	Ref [8]
$Ir_1/CoOOH_{sur}$	210	33	Ref [9]
Ir_1-$Ni(OH)_2$	260	78	Ref [10]
S-FeOOH/IF	244	59	Ref [11]
NiFe LDH-PMo12	206	47.5	Ref [12]
NiOOH/(LDH/α-FeOOH)	195	35	Ref [13]
Ru_1/D-NiFe LDH	189	31	Ref [14]
F-NiFe-A	218	32	Ref [15]
S/N-CMF@FexCoyNi_{1-x-y}-MOF	296	53.5	Ref [16]
Ir/CoFe-LDH/rGO,	195	48.6	Ref [17]
hBN-$NiFeO_xH_y$	230	30	Ref [18]
FeCoPBA-V_{CN}	218	39	Ref [19]
NiFe-S-TCNQ	209	36.1	Ref [20]

Reference

1. F. Wang, P. Zou, Y. Zhang, W. Pan, Y. Li, L. Liang, C. Chen and H. Liu, S. Zheng, *Nat. Commun.*, 2023, **14**, 6019.
2. T. H. M. Pham, T.-H. Shen, Y. Ko, L. Zhong, L. Lombardo, W. Luo, S. Horike, V. Tileli and A. Züttel, *J. Am. Chem. Soc.*, 2023, **145**, 23691.
3. C. Ni, H. Zheng, W. Liu, L. Wu, R. Li, K. Zhou and W. Zhang, *Adv. Funct. Mater.*, 2023, **33**, 2301075.
4. X. Li, H. Zhang, Q. Hu, W. Zhou, J. Shao, X. Jiang, C. Feng, H. Yang and C. He, *Angew. Chem. Int. Ed.*, 2023, **62**, 202300478.
5. Z. Zhang, C. Feng, D. Wang, S. Zhou, R. Wang, S. Hu, H. Li, M. Zuo, Y. Kong, J. Bao and J. Zeng, *Nat. Commun.*, 2022, **13**, 2473.
6. N. Zhang, Y. Hu, L. An, Q. Li, J. Yin, J. Li, R. Yang, M. Lu, S. Zhang, P. Xi and C. H. Yan, *Angew. Chem. Int. Ed.*, 2022, **61**, 202207217.
7. C. Zhang, Q. Qi, Y. Mei, J. Hu, M. Sun, Y. Zhang, B. Huang, L. Zhang and S. Yang, *Adv. Mater.*, 2022, **35**, 2208904.
8. Y. Wu, Y. Zhao, P. Zhai, C. Wang, J. Gao, L. Sun and J. Hou, *Adv. Mater.*, 2022, **32**, 2202523.
9. C. Feng, Z. Zhang, D. Wang, Y. Kong, J. Wei, R. Wang, P. Ma, H. Li, Z. Geng, M. Zuo, J. Bao, S. Zhou and J. Zeng, *J. Am. Chem. Soc.*, 2022, **144**, 9271.
10. Q. He, S. Qiao, Q. Zhou, Y. Zhou, H. Shou, P. Zhang, W. Xu, D. Liu, S. Chen, X. Wu and L. Song, *Nano Lett.*, 2022, **22**, 3832.
11. X. Chen, Q. Wang, Y. Cheng, H. Xing, J. Li, X. Zhu, L. Ma, Y. Li and D. Liu, *Adv. Funct. Mater.*, 2022, **32**, 2112674.
12. Z. Cai, P. Wang, J. Zhang, A. Chen, J. Zhang, Y. Yan and X. Wang, *Adv. Mater.*, 2022, **34**, 2110696.
13. M. Cai, Q. Zhu, X. Wang, Z. Shao, L. Yao, H. Zeng, X. Wu, J. Chen, K. Huang and S. Feng, *Adv. Mater.*, 2022, **35**, 2209338.
14. P. Zhai, M. Xia, Y. Wu, G. Zhang, J. Gao, B. Zhang, S. Cao, Y. Zhang, Z. Li, Z. Fan, C. Wang, X. Zhang, J. T. Miller, L. Sun and J. Hou, *Nat. Commun.*, 2021, **12**, 4587.
15. Q. Xu, H. Jiang, X. Duan, Z. Jiang, Y. Hu, S. W. Boettcher, W. Zhang, S. Guo and C. Li, *Nano Lett.*, 2021, **21**, 492.
16. Y. Zhao, X. F. Lu, Z. P. Wu, Z. Pei, D. Luan and X. W. D. Lou, *Adv. Mater.*, 2023, **35**, 2207888.
17. W. Xu, J. Cao, T. Mou, B. Mei, P. Yao, C. Han, X. Gong, P. Song, Z. Jiang, T. Frauenheim and J. Xiao, *Angew. Chem. Int. Ed.*, 2023, **62**, 202310973.
18. Y. Lu, B. Li, N. Xu, Z. Zhou, Y. Xiao, Y. Jiang, T. Li, S. Hu, Y. Gong and Y. Cao, *Nat. Commun.*, 2023, **14**, 6965.
19. Y. Lin, H. Ren, S. Zhang, S. Liu, T. Zhao, W. J. Jiang, W. Zhou, J. S. Hu and Z. Li, *Adv. Energy Mater.*, 2023, **14**, 2302403.
20. Y. Lin, J. Fang, W. Wang, Q. Wen, D. Huang, D. Ding, Z. Li, Y. Liu, Y. Shen and T. Zhai, *Adv. Energy Mater.*, 2023, **13**. 2300604.